General Disclaimer

One or more of the Following Statements may affect this Document

- This document has been reproduced from the best copy furnished by the organizational source. It is being released in the interest of making available as much information as possible.

- This document may contain data, which exceeds the sheet parameters. It was furnished in this condition by the organizational source and is the best copy available.

- This document may contain tone-on-tone or color graphs, charts and/or pictures, which have been reproduced in black and white.

- This document is paginated as submitted by the original source.

- Portions of this document are not fully legible due to the historical nature of some of the material. However, it is the best reproduction available from the original submission.

NASA TECHNICAL MEMORANDUM

NASA TM-73880

NASA TM-73880

COMPARISON OF THE NOISE CHARACTERISTICS OF TWO LOW PRESSURE RATIO FANS WITH A HIGH THROAT MACH NUMBER INLET

by Howard L. Wesoky, John M. Abbott, and Donald A. Dietrich
Lewis Research Center
Cleveland, Ohio 44135

January 1978

1. Report No. NASA TM-73880	2. Government Accession No.	3. Recipient's Catalog No.
4. Title and Subtitle COMPARISON OF THE NOISE CHARACTERISTICS OF TWO LOW PRESSURE RATIO FANS WITH A HIGH THROAT MACH NUMBER INLET		5. Report Date January 1978 6. Performing Organization Code
7. Author(s) Howard L. Wesoky, John M. Abbott, and Donald A. Dietrich		8. Performing Organization Report No. E-9489 10. Work Unit No.
9. Performing Organization Name and Address National Aeronautics and Space Administration Lewis Research Center Cleveland, Ohio 44135		11. Contract or Grant No. 13. Type of Report and Period Covered Technical Memorandum
12. Sponsoring Agency Name and Address National Aeronautics and Space Administration Washington, D.C. 20546		14. Sponsoring Agency Code

15. Supplementary Notes

16. Abstract

Acoustics data obtained in experiments with two low pressure ratio 50.8-cm (20-in.) diameter model fans differing in design tip speed were compared. Determination of the average throat Mach number used to compare high Mach inlet noise reduction characteristics was based on a correlation of inlet wall static pressure measurements with a flow field calculation. The largest noise reductions were generally obtained with the higher tip speed fan. At a throat Mach number of 0.79, the difference in noise reduction was about 3.5 dB with static test conditions. Although the noise reduction increased for the lower tip speed fan with a simulated flight velocity of 41 m/sec (80 knots), it was still about 2 dB less than that of the high tip speed fan which was only tested at the static condition. However, variations in acoustic performance could not be absolutely attributed to the different fan designs because of differences in inlet lip contours which resulted in small variations of peak wall Mach number and axial extent of supersonic and near-sonic flow.

17. Key Words (Suggested by Author(s))	18. Distribution Statement
High Mach inlet Fan inlet performance	Unlcassified - unlimited STAR Category 07

19. Security Classif. (of this report)	20. Security Classif. (of this page)	21. No. of Pages	22. Price*
Unclassified	Unclassified		

* For sale by the National Technical Information Service, Springfield, Virginia 22161

COMPARISON OF THE NOISE CHARACTERISTICS OF TWO LOW PRESSURE RATIO FANS WITH A HIGH THROAT MACH NUMBER INLET

by Howard L. Wesoky, John M. Abbott, and Donald A. Dietrich

Lewis Research Center

E-9489

SUMMARY

Acoustics data obtained in experiments with two low pressure ratio 50.8-cm (20-in.) diameter model fans differing in design tip speed were compared. Determination of the average throat Mach number used to compare high Mach inlet noise reduction characteristics was based on a correlation of inlet wall static pressure measurements with a flow field calculation. At the static test condition, an inlet throat Mach number of about 0.79 resulted in 3.5 dB more perceived noise reduction for the fan with the higher design tip speed. For a simulated aircraft speed of 41 m/sec (80 knots), the reduction of noise from the lower tip speed fan was about 2 dB less than for the higher tip speed fan of the static condition. However, variations in acoustic performance could not be absolutely attributed to the different fan designs (i.e., different noise source characteristics) because of differences between the inlet lips used in the two experiments. Small differences in peak wall Mach number and axial extent of the region of supersonic and near-sonic flow may have contributed to the variation of noise reduction characteristics.

INTRODUCTION

As part of the Quiet Clean Short Haul Experimental Engine (QCSEE) Project (ref. 1), a series of model experiments on component performance have been conducted. The characteristics of the QCSEE fan for the under-the-wing (UTW) propulsion system were investigated by the General Electric Company in the Research and Development Center Anechoic Chamber (refs. 2 and 3) where a 50.8-cm (20-in.) diameter model fan was tested with various inlet configurations at ground static conditions. Simulated in-flight engine inlet aerodynamic performance of some of the same inlet configurations was investigated in the NASA Lewis Research Center 9- by 15-Foot VSTOL Wind Tunnel (ref. 4) where a different fan was used. The anechoic character of the wind tunnel test section (refs. 5 and 6) also provided the opportunity to investigate and compare the simulated in-flight and static performance of these fan and inlet configurations (refs. 7 to 10).

Another opportunity provided by the anechoic chamber and wind tunnel experiments is the comparison of the noise reduction obtained with a high throat Mach number (i.e., nearly choked flow) inlet for two different low pressure ratio fans. Although this method of noise reduction, which provides the primary method for reduction of inlet radiated noise from the QCSEE propulsion systems, has been well demonstrated, the phenomenon is not well understood. The purpose of this report is to show the effect of a change in fan source noise on the noise reduction obtained with a high Mach inlet.

The QCSEE model fan of the anechoic chamber experiment had 18 rotor blades, a design tip speed of 306 m/sec (1005 ft/sec) and a design stage pressure ratio of 1.34 (ref. 2). Comparable characteristics of the model fan used in the wind tunnel experiment were 15 rotor blades, a design tip speed of 213 m/sec (700 ft/sec) and a design stage pressure ratio of 1.20 (refs. 4 and 9). Acoustic data were obtained for ranges of operating conditions in both cases, and various types of inlet noise reduction techniques were investigated in both experiments, including resonator type acoustic treatment, bulk absorber type acoustic treatment, and a combination of nearly choked flow with and without acoustic treatment. Only the noise reduction performance of inlets without acoustic treatment (i.e., "hard wall" inlets) will be considered here.

The baseline or unsuppressed acoustic performance was determined with a conventional inlet, called the "low Mach (LM) inlet," having a throat Mach number about 0.6 at its design weight flow. At this weight flow, the corresponding throat Mach number for the other inlet, called the "high-Mach (HM) inlet," was about 0.8. The noise reduction obtained from the high-Mach inlet was determined by comparing its performance to the "low-Mach (LM) inlet," at the same fan operating conditions.

The same inlet duct was used for the two experiments except for the lip contours. The bellmouth-type inlet lip used for most configurations of the static (i.e., no forward velocity) anechoic chamber experiment was designed to simulate the flow field of a flight-type inlet lip at a 41 m/sec (80 knots) aircraft speed. In the wind tunnel experiment, only a flight-type inlet lip was used. Flow field information obtained with both types of lips will be presented and compared.

Perceived noise levels and one-third octave band sound pressure levels will also be presented for both experiments. Tunnel velocities of 0 and 41 m/sec (80 knots) will be considered for the wind tunnel experiments. The model fans were operated over ranges of rotational speeds to vary the inlet weight flow and investigate the effect of throat Mach number on noise reduction.

APPARATUS

Test Facilities

Wind tunnel. - Aerodynamic test characteristics of the NASA Lewis 9- by 15-Foot V/STOL Wind Tunnel are provided in reference 11. Schematic representations of the model in the wind tunnel are shown in figures 1(a) and (b), and a photograph is shown in figure 1(c). Further discussion of the model installation will be given later.

A somewhat unique characteristic of the low speed test section is the ability to conduct anechoic experimentation in the acoustic direct field within the test section during tunnel operation. Details of the acoustic characteristics of the test section are reported in references 5 to 8 which indicate that anechoic or free field properties exist for frequencies above 1000 hertz. For the purposes of acoustic testing, the anechoic wind tunnel has the favorable characteristics of remote drive motors, an acoustical muffler between the compressor and test section, and acoustic treatment on the first turn upstream and downstream of the test section. The test section walls, floor and ceiling also have acoustic treatment. With these features, the background noise level (one-third octave band) in the test section is about 82 dB at 1000 hertz for a 41 m/sec (80 knots) airflow velocity. The background noise level is lower at lower airflow velocities and at higher frequencies (ref. 6). Small corrections made to the acoustic measurements to account for background noise are discussed in the Data Analysis Procedure section.

Anechoic chamber. - Figure 2 shows a schematic representation and photograph of the General Electric Research and Development Center Anechoic Chamber. Some of the data for the comparison to be reported here (refs. 2 and 3) were obtained in this facility. The fan engine model is shown installed in the anechoic chamber which is approximately 10.7 m (35 ft) wide by 7.6 m (25 ft) long by 3.1 m (10 ft) high. All walls, floor and ceiling are covered with foam wedges. The standing wave ratio at 200 hertz is less than ±1 dB. Porous walls are used for minimum inflow distortion to the fan when measuring inlet radiated noise.

Model Fans

Characteristics of the two 50.8-cm (20-in.) diameter model fans are given in table I. The lower pressure ratio fan used in the wind tunnel experiment will be referred to as Rotor 55, and is seen to have fewer rotor blades and stator vanes as well as a lower design rotational speed than the QCSEE UTW model

fan. Further details of the fan designs are given in references 4 and 12 for Rotor 55, and in references 2 and 13 for the QCSEE model. Although both fans had a variable pitch capability, only the design blade angles will be considered in this report.

Rotor 55. - The acoustic properties of Rotor 55 are discussed in reference 8 which notes that, for the stator vane-to-rotor blade ratio of 1.67, the theory of tone cut-off predicts that the fundamental or first harmonic of the blade passage tone will not propagate below 107 percent of the design speed. This cut-off speed was calculated for conditions at the throat of the "low Mach (LM) inlet." However, according to reference 7, this theory does not consider any effect of the rate of inlet radius contraction, which may account for the cut-off effect being observed over a larger range of fan speeds than predicted, as noted in references 7 and 8.

Rotor 55 was driven by an axial flow turbine which used air as the driving fluid. Drive air was delivered to the turbine plenum through the vertical model support and pylon as indicated in figure 1(a). Fan and turbine discharge flows were ducted through a 90° elbow to an acoustic muffler, and exhausted outside the test section (ref. 4). An adjustable plug at the muffler exit allowed the remote setting of the exhaust nozzle area and, thereby, the fan operating point. The 90° elbow and vertical duct were lined with acoustic treatment to suppress aft fan noise. In addition, turning vanes in the elbow were acoustically treated to prevent reflection of aft fan noise upstream. As shown in figure 1, the inlet angle (to the tunnel flow) could be varied by rotating the model in the horizontal plane, but all tests reported herein were made with zero inlet flow angle. Flow angle effects on noise are reported in references 4, 7, and 9 for the configurations considered here.

QCSEE fan. - Acoustic characteristics for the QCSEE UTW model fan are discussed in reference 2. Its design was not based on the theory of tone cut-off. An electric motor (fig. 2) was used to drive this fan, and its discharge air was split into simulated bypass and core flow streams. As explained in reference 13, the bypass flow was ducted radially outward through a cylindrical ring discharge valve and exhausted through a stack outside the anechoic chamber. The core flow was collected in a manifold and exhausted by pumps outside the test chamber. No acoustic treatment was included in the discharge duct of the QCSEE fan model.

Model Inlets

Model inlet characteristics are given in table II and figure 3. Many of the inlet components were common to the two experiments. In particular, the duct

wall contours between the diffuser entrance, that is, inlet throat, and the diffuser exit were identical. Only flight type inlet lips were used in the wind tunnel experiment with Rotor 55. The inlet lips used for most configurations of the QCSEE fan experiment in the anechoic chamber were designed to simulate the flow field of flight type inlet lips at a 41 m/sec (80 knots) aircraft speed, and will be referred to as aeroacoustic lips. A comparison of the flight and aeroacoustic lips is shown in figure 3(b) for the high Mach inlet (HM). Similar lips were used for the low Mach inlet (LM). The information of table II and figure 3(a) pertains only to the flight lips. Coordinates of the aeroacoustic lips are provided in reference 2.

Figure 3(b) also shows that the centerbodies for the two fans had different contours and that the fan faces were at different axial planes. These differences did not affect the aerodynamic flow fields in the upstream end of the inlets, particularly near the throat where noise propagation is presumed to be controlled by the high Mach inlet (HM).

Instrumentation

Aerodynamic. - Pressure and temperature rakes used to measure fan aerodynamic performance are described in references 4 and 9 for Rotor 55, and in references 2 and 13 for the QCSEE fan. Total pressure rakes used to measure inlet pressure recovery and distortion are also described in the same references. However, because of the excellent inlet performance, typified by total pressure recoveries greater than 0.99 for the conditions of this report (ref. 4), only wall static pressure distributions measured with appropriate inlet wall mounted instruments will be considered here.

Acoustic. - Microphone instrumentation used for the Rotor 55 wind tunnel experiment is described in reference 9. Only results obtained with the sword microphone shown in figure 1(c) will be considered here. This microphone was located 3.6 fan diameters from the intersection of the fan axis with the inlet highlight plane and was mounted on the end of a boom which rotated about a vertical axis through the inlet face in a circular arc at the height of the fan axis. The very thin streamlined microphone assembly weathervaned above its support, always oriented directly with the tunnel airflow, which is the condition of minimum wind noise on the microphone. Sound pressure signals from the microphone used here were conditioned in a conventional manner and recorded on magnetic tape.

Microphone instrumentation used for the QCSEE fan model experiment in the anechoic chamber is described in reference 2. Only results obtained from 12 fixed microphones located on a 5.2 m (17 ft) arc from 0^{o} to 110^{o} relative to the

inlet axis (fig. 2(a)) will be considered here. All of the microphones were continuously monitored on oscilloscopes, and the signals recorded on magnetic tape.

PROCEDURE

Detailed explanations of the conditions and procedures used for the acquisition of aerodynamic and acoustic performance data are given in references 4, 7, 8, and 9 for the Rotor 55 experiment; and in references 2 and 13 for the QCSEE fan experiment.

Test Conditions

Data obtained at wind tunnel airflow velocities of 0 and 41 m/sec (80 knots) will be considered here. The tunnel flow case corresponds to the typical aircraft takeoff and landing speed chosen for the QCSEE Project. Fixed fan rotational speeds, between 90 and 110 percent of the design corrected speed, were used and nozzle area was only varied slightly to maintain a fixed operating line (i.e., fan pressure ratio vs. weight flow relationship).

In the anechoic chamber experiment with the QCSEE model fan, three parameters were varied; model fan rotational speed, fan exit area, and rotor blade angle. The effects of exit area and rotor blade angle are discussed in references 2 and 13. Fixed fan rotational speeds, between 90 and 103 percent of the design corrected speed, will be considered here.

Data Analysis Procedure

As previously indicated, all of the acoustics data presented here were recorded on magnetic tape. One-third-octave band analysis was performed later with commercially available analyzers. Model sound pressure level spectra obtained with tunnel flow were then corrected for background noise, which was generally less than 2 dB and only significant at frequencies near 1000 hertz. Frequencies below 1000 hertz were not considered in the data analysis because, as previously indicated in the APPARATUS section, the wind tunnel test section is not anechoic for lower frequencies. Background noise spectra are presented in reference 9.

Noise data were extrapolated to a 152 m (500 ft) sideline and adjusted to FAR-36 standard conditions of 298 K (77° F) and 70 percent relative humidity

using computerized methods.* Model sound pressure levels were adjusted to a level equivalent to the full scale QCSEE propulsion system (ref. 1) by using the ratio of engine-to-model fan tip circumscribed areas (i.e., diameter squared) which was 12.60. Therefore, according to standard logarithmic scaling relations, an increment of 11.0 dB was added to the model sound pressure levels.

In the scaling procedure, frequencies of the model noise data were shifted downward to obtain the engine scale spectra through consideration of the engine-to-model fan diameter ratio, 3.55, and the blade passage frequency. Using the diameter ratio, the frequency shift was determined precisely, but the actual shift was dependent on the position of the blade passage frequency within a one-third-octave band. Shifts of five or six one-third-octave bands were applied to the data reported here. Finally, perceived noise levels were calculated for the scaled and extrapolated microphone data using a computerized procedure based on the requirements of FAR-36.

It should also be noted that the QCSEE fan anechoic chamber model data from reference 3 were used rather than the engine scale data from that reference because the engine scale data include the effect of extra ground attenuation, which is not considered here.

RESULTS AND DISCUSSION

Fan Aerodynamic Performance

Fan maps are shown in figures 4 and 5 which indicate the operating lines used for the acoustic experiments with Rotor 55 and the QCSEE fan. These data are based on information obtained in the aerodynamics portions of the experiments; reported in reference 4 for Rotor 55, and references 2 and 12 for the QCSEE fan. Rakes used for the aerodynamic measurements were, of course, removed for the acoustic experiments. The relatively low stage total pressure ratios indicated for the fans are representative of very high bypass ratio turbofan engines and are typical of those recently considered for application to short takeoff and landing (STOL) transport aircraft (ref. 14).

---

*Private communication from F. J. Montegani. Unpublished computer program for band attenuations by numerical integration using pure-tone atmospheric attenuation results from NASA CR-2760. Program available on request.

Inlet Throat Mach Number Determination

General. - Average inlet throat Mach number was used as the correlating parameter for comparison of acoustics data from the two experiments because of its importance in characterizing the noise reduction capabilities of high Mach inlets. However, this parameter is very sensitive to small changes in inlet weight flow; as typified by a rate of change for Mach number three times greater than that for weight-flow near a Mach number of 0.8. As indicated in references 2 and 9, the perceived noise radiated from a high Mach inlet typically varies about 1 dB for each 1 percent change in throat Mach number near a throat Mach number of 0.8. Therefore, at this representative throat Mach number for high Mach inlet performance, a 1 percent variation in inlet weight flow can result in a 3 dB change in inlet radiated noise.

Throat Mach number and weight flow were initially determined with different techniques in the two experiments considered here. In the wind tunnel experiment with Rotor 55, the plug nozzle of the acoustic muffler (fig. 1) was calibrated to measure weight flow as described in reference 4. In the anechoic chamber experiment with the QCSEE fan, inlet wall static pressure measurements were correlated with throat Mach number and weight flow from a computerized compressible flow analysis (ref. 2). This technique, called the Stream Tube Curvature (STC) program (ref. 15), also involved a boundary layer correction to the inviscid calculation.

Comparability of the two throat Mach number measurement techniques was determined by application of the calibration procedure from the QCSEE fan experiment to the Rotor 55 experiment. General results of this exercise are shown in figure 6 for inlet HM with a flight lip, used in the Rotor 55 experiment. Throat Mach number determined from the nozzle calibration, M_{TH}, is compared to a throat Mach number determined from the STC inlet flow calibration, $M_{TH,STC}$. The nozzle calibration generally resulted in a higher estimate of the throat Mach number than the STC calibration, with the difference increasing with increasing Mach number. At a throat Mach number, M_{TH}, of 0.80; the STC calibration estimate of the Mach number, $M_{TH,STC}$, was about 0.77. This variation in Mach number is analogous to a slightly greater than 1 percent variation in inlet weight flow. It should be noted that the STC aeroacoustic lip calibration data were applied to the flight lip experiment with tunnel flow because flight lip calibration data were not available for the tunnel flow case, and, also, the aeroacoustic lip at static conditions was designed to simulate the flight lip flow field at 41 m/sec (80 knots) according to reference 2.

Application. - Because it is not possible at this time to determine which of the throat Mach number measurement techniques is most accurate, it was

decided to use the STC calibration to correlate acoustic results from the two experiments. This was done to maintain consistency of data analysis for the two experiments, and to possibly eliminate throat Mach number measurement error as a source of variation between acoustic results.

Figures 7 and 8 show examples of the STC correlation application to the experiments. The procedure followed, as explained in reference 2 where the analytical results were obtained, was to specify inlet wall static pressure tap locations near the inlet throat and then to calculate the static pressure relationship to throat Mach number for these locations. Results of these calculations are indicated in figures 7 and 8 for a wide range of throat Mach number. The region slightly downstream of the throat was chosen for the calibration because of the high sensitivity of static pressure to weight flow variation in this region of the inlet.

The next step in the calibration procedure was to relate the experimental measurements of static pressure at the appropriate locations to the STC flow correlation results to determine throat Mach number, $M_{TH,STC}$, for a specific case. If the calibration procedure was absolutely correct, correlation of experimental data with the STC analysis should result in the same value of throat Mach number, $M_{TH,STC}$, for each pressure tap location. However, as indicated in figures 7 and 8, some scatter resulted. Although reference 2 attributes this scatter to model contour inaccuracies, imprecise tap installations or undetected leaks in the pressure lines; inaccuracy of the STC flow analysis may also be a cause of the scatter.

Figure 7, which considers a Rotor 55 case for no wind tunnel flow, indicates that deviations from the indicated average throat Mach number were equivalent to as much as 1.8 percent of inlet weight flow. Figure 8, which considers cases where Rotor 55 and the QCSEE fan had the same calibrated throat Mach number, indicates somewhat less scatter than figure 7, but shows the same amount of scatter resulted for the two experiments. The inlet of the QCSEE fan referred to in figure 8 as inlet HMB had the same contour as inlet HM, but with acoustic treatment in the diffuser. As noted in reference 4, this had a negligible effect on the inlet aerodynamic performance, and is considered here only as a case which can be conveniently compared to the Rotor 55 experiment.

Therefore, although the accuracy of the technique may be questioned, the STC flow correlation procedure was used as the basis for comparison of the acoustic data for the two experiments with inlet HM. For inlet LM, where the throat Mach number was never larger than 0.63, no attempt was made to redefine the values originally reported for the two experiments. Although figure 6 applies directly only to inlet HM, it is representative of the good agreement

between different methods of throat Mach number measurement for the levels of inlet LM (i.e., <0.63).

Comparison of Inlet Flow Fields

As previously indicated, the aerodynamic flow fields reported in reference 2 for the inlets with aeroacoustic lips tested at static conditions were stated to be equivalent to the flow fields for inlets with flight lips and an aircraft velocity of 41 m/sec (80 knots). Results of a STC flow analysis at the design throat Mach number of 0.79 were used to justify this conclusion. These results were presented in a figure similar to figure 9 which shows calculated wall Mach number as a function of axial location for the flight lip with wind tunnel flow and for the aeroacoustic lip at static conditions.

Downstream of the throat (zero axial location) the results compare very well. However, upstream of the throat, where the lip contours diverge as indicated in figure 3(b), significant differences do seemingly exist between the calculated flow fields. The calculation results are shown to be discontinuous immediately upstream of the throat to indicate the actual gap in the calculation procedure which makes comparison of wall Mach number peaks difficult. Because the envelope of flight lip results is within the envelope of aeroacoustic lip results near the discontinuities, it could be postulated that the aeroacoustic lip has a higher peak wall Mach number than the flight lip. If this is true, then, not only would the flow fields be aerodynamically dissimilar, but different acoustic characteristics would also result. In particular, dissimilar velocity peaks would be expected to affect the relative noise suppression characteristics of the aeroacoustic and flight lips. However, the weight flow or throat Mach number calibrations are not affected significantly because STC calculations from the immediate vicinity of the peaks were not used for the correlations (figs. 7 and 8).

Comparisons of measured wall Mach number distributions from the two experiments are shown in figures 10 and 11. In figure 10, data are compared at near inlet design weight flow conditions to indicate the degree of flow field similarity for the aeroacoustic lip, flight lip without tunnel flow and flight lip with tunnel flow. Downstream of the Mach number peaks, the distributions are similar except for two axial locations, about 0.16 and 0.59, for the QCSEE fan experiment where the pressure taps may have leaked. The peak for the aeroacoustic lip was slightly higher than those for the flight lip, which may be indicative of a higher weight flow as shown by the relative values of $M_{TH,STC}$, or the relative locations of the pressure taps for the two inlets. However, an actual difference in peak wall Mach number is certainly possible, as suggested in the previous discussion of figure 9.

Peak values of the wall Mach numbers were nearly equal for the flight lip with and without tunnel flow, indicating that, in terms of the peak Mach number, the flight lip at static conditions simulated the flight lip at 41 m/sec (80 knots). For the same flight lip, significant variations in wall Mach number occurred upstream of the peaks between tunnel off and on conditions, which indicates the variation of the inlet streamtube with flight speed. Differences in the wall Mach number between flight and aeroacoustic lips upstream of the peak values are, of course, attributable to the variation in lip contours. Even though these differences in aerodynamic performance can be correlated with area variation, the indicated differences in axial Mach number gradients between lips upstream of the peak values can be important to acoustic performance.

Although the near sonic and supersonic flow regions downstream of the peaks may be more important for noise reduction than the upstream flow regions, the upstream regions may have some effect. Refractive effects caused by the transonic flows or by the different lip contours could affect both the level and directivity of the inlet radiated noise. The significance of the flow field variations in the upstream region on the radiated noise cannot be accurately evaluated at this time, but will be considered when evaluating acoustic results.

Figure 11 compares wall Mach number distributions obtained for the two fans with exactly the same inlet HMB, including lip contours. As noted in the discussion of figure 8, inlet HMB had the same contour as inlet HM, but with acoustic treatment in the diffuser; and is used here because it was the only flight lip configuration used in both experiments. The results shown in figure 11 indicate that a high degree of flow field similarity existed for the two experiments, as would be expected for identical inlet configurations, even with different fans. The generally small differences in Mach number that occurred throughout the inlet can, of course, be attributed to the small weight flow variation indicated by the throat Mach numbers shown with the figure.

Comparison of Acoustic Performance

Perceived noise levels and reduction characteristics. - Figure 12 shows a comparison of QCSEE fan perceived noise levels as function of fan speed for both inlets LM and HM. Directivity results presented in reference 2 indicate that peak noise levels occurred at the 60° angle noted on the figure. At 90 percent fan speed, the noise levels from the two inlets were almost equal, but, as fan speed was increased, the inlet LM noise level remained relatively constant while the inlet HM noise level decreased significantly. This, of course, was a result of high throat Mach number which will be further discussed later.

Figure 13 shows similar perceived noise level variation with rotational speed for Rotor 55. These engine scale results for inlets LM and HM were also obtained at 60^{o} from the centerline where near peak noise levels occurred for this fan as indicated in reference 9. The effect of simulated forward velocity, also as reported in reference 9, is indicated by the 2 to 3 dB lower noise levels shown for the case of wind tunnel flow relative to the static case. As previously shown for the QCSEE fan, the Rotor 55 noise levels for the two inlets are about equal at the lowest fan speeds. However, the Rotor 55 results for inlet LM indicate a small reduction of noise level with increasing fan speed which is a characteristic of the fan noise source. The inlet HM noise variation with fan speed is much more significant, once again indicating the effect of high throat Mach number, which is shown more directly in the next figure.

Figure 14 presents the same noise data as figures 12 and 13 with fan speed replaced by throat Mach number. As previously noted for Rotor 55, only the inlet HM throat Mach numbers were actually determined with the STC correlation procedure indicated by $M_{TH,STC}$ in figure 14, since inlet LM throat Mach numbers were relatively insensitive to measurement procedure. Comparison of the engine scale data shows that the QCSEE fan had a much higher noise level than Rotor 55; about 6 dB or more for the baseline low Mach inlet. This result might be expected because of the relative fan design characteristics, with the QCSEE fan having a higher tip speed and higher stage pressure ratio.

The noise reduction characteristics of the high throat Mach number inlet are clearly indicated in figure 14 for both fans, where the variations of noise level with throat Mach number have been approximated with least square parabolas. Large reductions in noise level were experienced with both fans as inlet HM throat Mach number was increased. However, the rate of noise reduction appears to have been higher for the QCSEE fan than for Rotor 55. At a throat Mach number of about 0.65 the difference in static noise level between the QCSEE fan and Rotor 55 was about 6.5 dB, but at a throat Mach number of about 0.79 the difference was only about 4.5 dB. A similar relationship exists between the static QCSEE fan noise levels and the Rotor 55 noise levels with tunnel flow.

Variations of a noise reduction parameter with inlet HM throat Mach number are shown in figure 15 for the same configurations and test conditions as the previous figure. Least square parabolas were again used to approximate the variations of the parameter, which is defined as the difference between inlet LM and HM noise levels for the same fan speed. As implied from the previous figure, the reductions of noise from the QCSEE fan were greater than with Rotor 55. At a throat Mach number of 0.79, the QCSEE fan noise reduction was about 10 dB; while the Rotor 55 noise reduction was about 6.5 dB without tunnel flow and 8 dB

with tunnel flow. Based on the data reported here and in reference 9 for Rotor 55, it might be expected that the QCSEE fan noise reductions would be even larger with forward velocity.

Although tunnel flow has been shown to increase the noise reduction capability of the high Mach inlet with Rotor 55, the magnitude of the effect approaches the accuracy limitation of the instrumentation noted in reference 10, about 1 dB for absolute levels and 2 dB for differences between levels. In reference 10, an attempt to reduce this uncertainty was made by adjusting the inlet LM data for no tunnel flow by using very low frequency noise measurements as a supplemental calibration of the system. The adjustment was somewhat subjective and, therefore, was not used in this study. The result of the reference 10 adjustment was to decrease the difference in level between the inlet LM noise with and without tunnel flow. Such adjustments would reduce by 1 to 2 dB the high Mach inlet noise reduction without tunnel flow and, thus, increase the effect of tunnel flow on the perceived noise reduction capability of inlet HM with Rotor 55. The adjustment would also increase the difference between the noise reductions observed with the QCSEE fan and Rotor 55 at static conditions, and, therefore, indicates that the results of figure 15 are least qualitatively correct and significant. The measured equivalence of Rotor 55 noise levels for inlets LM and HM at the lowest fan speeds and throat Mach numbers (figs. 13 and 14) does tend to support, however, the data analysis procedure of this report.

Even though the results of figure 15 can be supported on a qualitative basis, the variations in high Mach inlet noise reduction between the experiments cannot be absolutely attributed to the different fans because of the flow field variations between the aeroacoustic and flight lips. As previously indicated, the flow fields have many important similarities. However, the larger region of supersonic and near-sonic flow for the flight lip shown in figure 10 might even suggest a noise reduction advantage for this case relative to the aeroacoustic lip, opposite to what is indicated in figure 15. Effects such as noise refraction, which also affect the noise reduction characteristics, must be examined to help understand the relative importance of the fan noise sources and inlet lip contours.

Sound pressure level spectra and reduction characteristics. - Typical sound pressure level (SPL) and reduction spectra are shown in figure 16 for the QCSEE fan, in figure 17 for Rotor 55 without tunnel flow and in figure 18 for Rotor 55 with tunnel flow. Near inlet design weight flow conditions are considered in each case, and the SPL reduction spectra simply represent the difference between appropriate inlet LM and HM SPL's.

Figure 16 indicates that the high Mach inlet reduced the QCSEE fan SPL at all frequencies, with a moderate increase in reduction capability with increasing frequency. The apparently large selective SPL reduction at 1250 hertz was

caused by a problem of acoustic energy at the blade passage frequency (BPF) being shared by two one-third-octave filters, as indicated by the relatively flat inlet LM spectrum between 1000 and 1250 hertz.

Figure 17 indicates that the high Mach inlet also reduced the Rotor 55 SPL at all frequencies for the case without tunnel flow. No monotonic variation of SPL reduction with frequency was noted for Rotor 55. At low frequencies, the amounts of SPL reduction for Rotor 55 and the QCSEE fan (fig. 16) were similar, with the differences possibly attributable to the variation of throat Mach number. However, at high frequencies, Rotor 55 experienced considerably less SPL reduction. This, therefore, must affect the difference in perceived noise reduction observed for the two fans, because of the selective weighting involved in the perceived noise calculation which emphasizes the high frequencies in the scaled result. Although the throat Mach numbers are slightly different for the data of figures 16 and 17, the variations of SPL with frequency are typical.

Figure 18 indicates that, with wind tunnel flow, a slight increase in Rotor 55 high Mach inlet noise reduction with increasing frequency was noted, as well as a small selective increase of noise reduction at the third harmonic of the blade passage frequency. However, the reduction level does not approach that obtained with the QCSEE fan at high frequencies (fig. 16). The cut-off effect on the tone of the blade passage frequency that occurred with tunnel flow can be noted in figure 18 by comparison with the previous figure which considered the static case. This phenomenon has been previously discussed in references 7 and 8, and, therefore, it will only be noted here that its observation is evidence of the wind tunnel's usefulness for simulation of atmospheric flight.

Further discussion of Rotor 55 sound pressure level spectra are given in references 7 to 10. In particular, reference 9 showed that, as a comparison of figures 17 and 18 would indicate, Rotor 55 SPL was reduced across the spectrum with tunnel flow. However, the results of reference 7, which were obtained with a different fan operating line, did indicate some tone and broadband increases of SPL with tunnel flow. Also, the adjustment of the inlet LM spectra without tunnel flow used in reference 10 would, if correct, eliminate some of the broadband effects indicated in reference 9 or by a comparison of figures 17 and 18. Therefore, a generalized relationship between SPL and tunnel velocity is not apparent. Further discussion of QCSEE fan sound pressure level spectra is given in reference 2.

SUMMARY OF RESULTS

Acoustic data obtained in experiments with two low pressure ratio 50.8-cm (20-in.) diameter model fans were compared. Determination of the average

throat Mach number used to compare high Mach inlet noise reduction characteristics was based on a correlation of inlet wall static pressure measurements with a flow field calculation. At the static test condition, an inlet throat Mach number of about 0.79 resulted in 3.5 dB more perceived noise reduction for the fan having 18 rotor blades and a design tip speed of 306 m/sec (1005 ft/sec) than for the fan having 15 rotor blades and a design tip speed of 213 m/sec (700 ft/sec). For a simulated aircraft speed of 41 m/sec (80 knots), the reduction of low tip speed fan noise was about 2 dB less than for the high tip speed fan at the static condition.

These observed variations in high Mach inlet noise reduction characteristics cannot be absolutely attributed to the different fan noise sources because of differences between the inlet lips used in the two experiments. A flight-type lip was used for the low tip-speed fan experiment conducted in an anechoic wind tunnel; whereas a more rounded, almost bellmouth, lip was used for the high tip-speed fan experiment in an anechoic chamber to simulate a flow field for an aircraft having forward speed. Small differences in peak wall Mach number and axial extent of the region of supersonic and near-sonic flow may have contributed to the variation of noise reduction characteristics.

The spectral characteristics of the high tip speed fan noise clearly indicated more high Mach inlet sound pressure level reduction at high frequencies than at low frequencies. Similar behavior was not apparent for the low tip speed fan without tunnel flow, and only a very slight increase of sound pressure level reduction with increasing frequency occurred with tunnel flow.

REFERENCES

1. Ciepluch, Carl C.: A Review of the QCSEE Program. NASA TM X-71818, 1975.

2. Bilwakesh, K. R.; and Clemons, A.: Acoustic Tests on a 20-Inch (50.8-cm) Diameter Scale Model (1:3.5) Fan and Inlet for the Under-the-Wing Engine. Vol. I, NASA CR-135117, 1978.

3. Bilwakesh, K. R.; and Clemons, A.: Acoustic Tests on a 20-Inch (50.8-cm) Diameter Scale Model (1:3.5) Fan and Inlet for the Under-the-Wing Engine. Vol. II, NASA CR-135118, 1978.

4. Abbott, John M.; Diedrich, James H.; and Williams, Robert C.: Low Speed Aerodynamic Performance of 50.8-Centimeter Diameter Noise Suppressing Inlets for the Quiet, Clean, Short-Haul Experimental Engine (QCSEE). NASA TP-1178, 1978.

5. Diedrich, J. H.; and Luidens, R. W.: Measurement of Model Propulsion System Noise in a Low-Speed Wind Tunnel. AIAA Paper 76-91, Jan. 1976.

6. Rentz, Peter E.: Softwall Acoustical Characteristics and Measurement Capabilities of the NASA Lewis 9×15 Foot Low Speed Wind Tunnel. (BBN-3176, Bolt, Beranek, and Newman, Inc.; NASA Contract NAS3-19410.) NASA CR-135026, 1976.

7. Dietrich, D. A.; Heidmann, M. F.; and Abbott, J. M.: Acoustic Signatures of a Model Fan in the NASA-Lewis Anechoic Wind Tunnel. AIAA PAPER 77-59, Jan. 1977.

8. Heidmann, M. F.; and Dietrich, D. A.: Simulation of Flight Type Engine Fan Noise in the NASA-Lewis 9×15 Anechoic Wind Tunnel. NASA TM X-73540, 1976.

9. Wesoky, Howard L.; Dietrich, Donald A.; and Abbott, John M.: Simulated Flight Effects on the Noise Characteristics of a High Throat Mach Number Fan Inlet. NASA TP-1199, 1978.

10. Heidmann, M. F.; and Dietrich, D. A.: Effects of Simulated Flight on Fan Noise Suppression. AIAA Paper 77-1334, Oct. 1977.

11. Yuska, J. A.; Diedrich, J. H.; and Clough, N.: Lewis 9- by 15-Foot V/STOL Wind Tunnel. NASA TM X-2305, 1971.

12. Lewis, George W., Jr.; and Tysl, Edward R.: Overall and Blade-Element Performance of a 1.20-Pressure Ratio Fan Stage at Design Blade Setting Angle. NASA TM X-3101, 1974.

13. Griffin, R. G.: McFalls, R. A.; and Beacher, B. F.: Aerodynamic and Aeromechanical Performance of a 50.8 Cm (20 In.) Diameter 1.34 PR Variable Pitch Fan with Core Flow. (R75AEG445, General Electric Co.; NASA Contract NAS3-18021.) NASA CR-135017, 1977.

14. Luidens, Roger W.; et al.: Engine Noise Technology. STOL Technology. NASA SP-320, 1972, pp. 371-412.

15. Keith, J. S.; et al.: Analytical Method for Predicting the Pressure Distribution About a Nacelle at Transonic Speeds. NASA CR-2217, 1973.

TABLE I. - 50.8-cm (20-in.) MODEL FAN CHARACTERISTICS

	QCSEE UTW[a]	Rotor 55
Number of rotor blades	18	15
Number of stator vanes	33	25
Vane-blade ratio	1.83	1.67
Rotor-stator spacing, true rotor tip chords	1.5	1.0
Hub-tip radius ratio	0.443	0.46
Rotor tip solidity	0.95	0.91
Rotor hub solidity	0.98	1.20
Design point:		
Corrected tip speed, m/sec (fps)	306 (1005)	213 (700)
Corrected fan speed, rpm (%)	11 520 (100)	8020 (100)
Fan stage pressure ratio	1.34	1.20
Corrected fan weight flow, kg/sec (lb/sec)	32.4 (71.4)	31.2 (68.8)
Fan adiabatic efficiency, %	88	90
Blade passage frequency, Hz	3456	2005

[a]Quiet Clean Short Haul Experimental Engine, Under-the-Wing propulsion system.

TABLE II. - CHARACTERISTICS OF INLETS WITH FLIGHT LIPS

Geometric variable	Low Mach (LM) inlet	High Mach (HM) inlet
(a) Internal lip		
Contraction ratio, $(D_{h\ell}/D_{TH})^2$	1.46	1.46
Surface contour	Ellipse	Ellipse
Proportions, a/b	2.0	2.0
(b) External forebody		
Diameter ratio, $D_{h\ell}/D_{max}$	0.880	0.900
Length-to-maximum diameter ratio, c/D_{max}	0.310	0.219
Surface contour	[a]DAC-1	[a]DAC-1
Proportions, c/d	5.166	4.380
(c) Diffuser		
Ratio of exit flow area to inlet flow area, $(D_e/D_{TH})^2$	1.283	1.466
Ratio of length to exit diameter, L_d/D_e	0.850	0.856
Maximum local wall angle, λ_{max}, deg	8.7	8.7
Location of maximum local wall angle, percent L_d	33.8	50.0
Surface contour	Cubic	Cubic
(d) Overall		
Inlet length-to-diffuser exit diameter ratio, L/D_e	1.035	1.029
(e) Rotor 55 centerbody		
Length-to-diffuser exit diameter ratio, L_c/D_e	0.267	0.267
Surface contour	[b]NACA-1	[b]NACA-1
(f) QCSEE fan centerbody		
Length-to-diffuser exit diameter ratio, L_c/D_e	0.227	0.227
Surface contour	(c)	(c)

[a]Douglas Aircraft Co. DAC-1 contour $(y/d)^2 = 2.318\ (x/c) - 2.748\ (x/c)^2 + 2.544\ (x/c)^3 - 1.113\ (x/c)^4$.

[b]Baals, D. D.; Smith, N. F.; and Wright, J. B.: The Development and Application of High-Critical-Speed Nose Inlets. NACA TR-920, 1948.

[c]Bilwakesh, K. R.; and Clemons, A.: Acoustic Tests on a 50.8-cm (20-in.) Diameter Scale Model (1:3.5) Fan and Inlet for the Under-the-Wing Engine, Vol. I, NASA CR-135117, 1978.

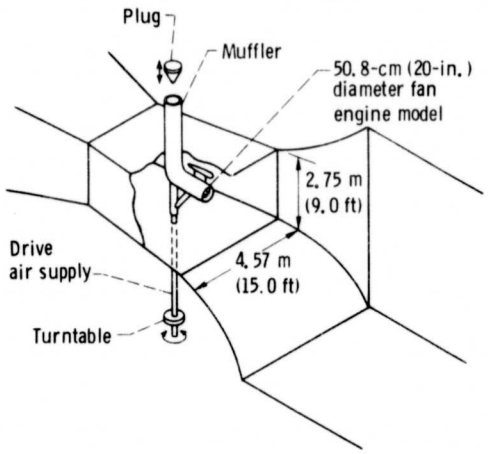

(a) Schematic view of 9- by 15-foot V/STOL windtunnel showing model installation.

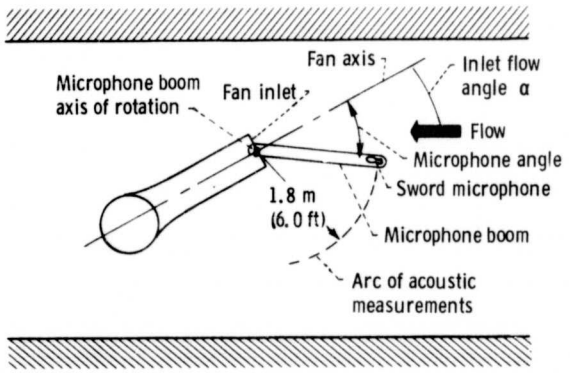

(b) Schematic plan view of 9x15-foot V/STOL wind tunnel test section.

Figure 1. - NASA Lewis experimental facility.

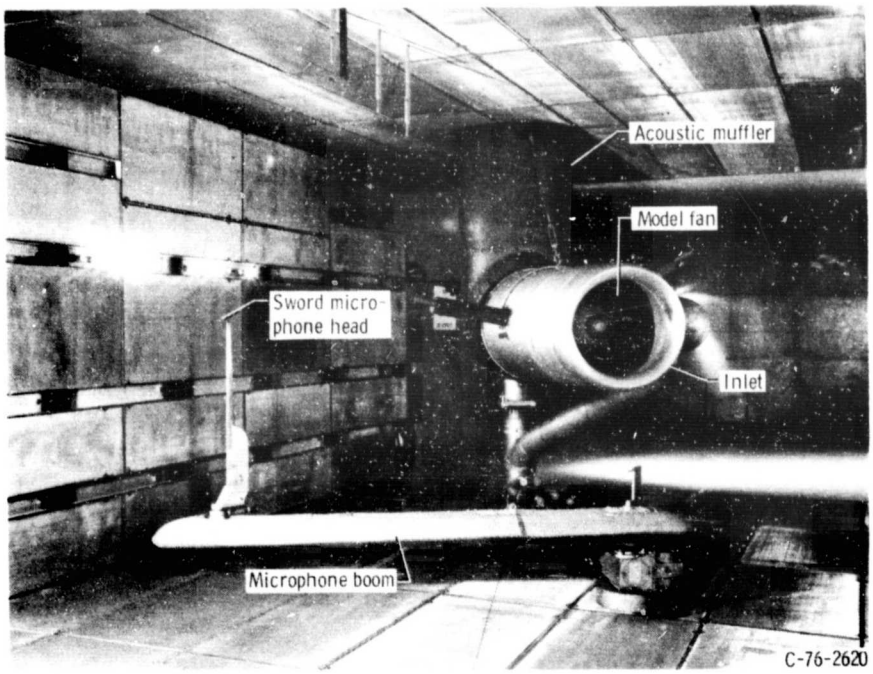

(c) Photograph of fan engine model in test section looking downstream.

Figure 1. - Concluded.

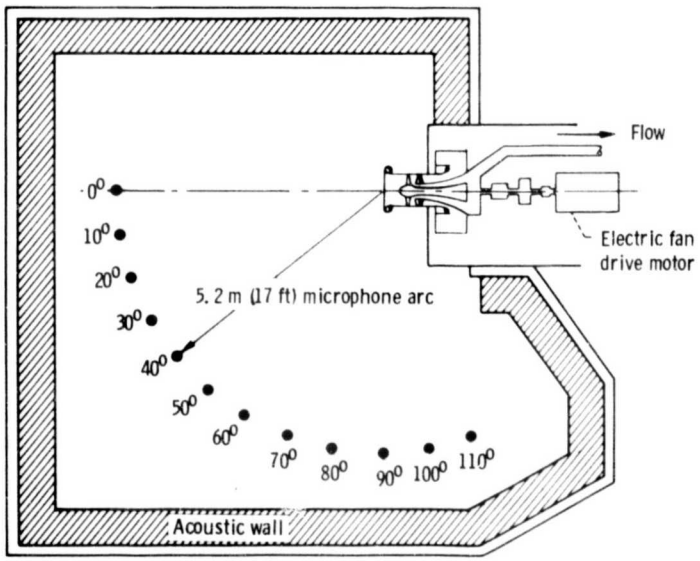

(a) Schematic plan view.

Figure 2. - General Electric Research and Development Center anechoic chamber.

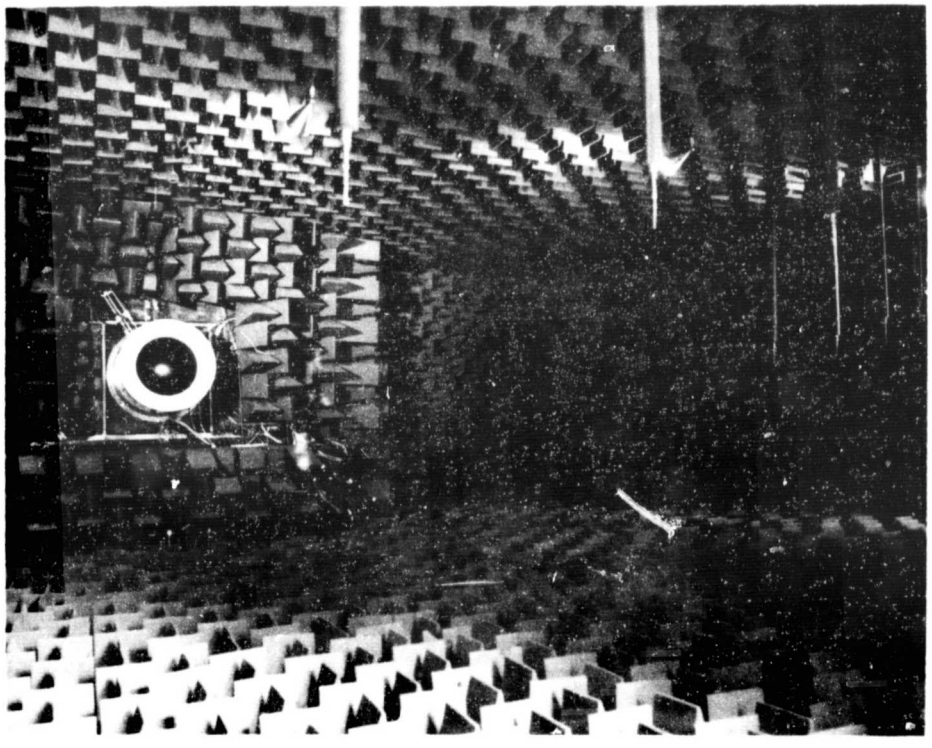

(b) Photograph of test facility.

Figure 2. - Concluded.

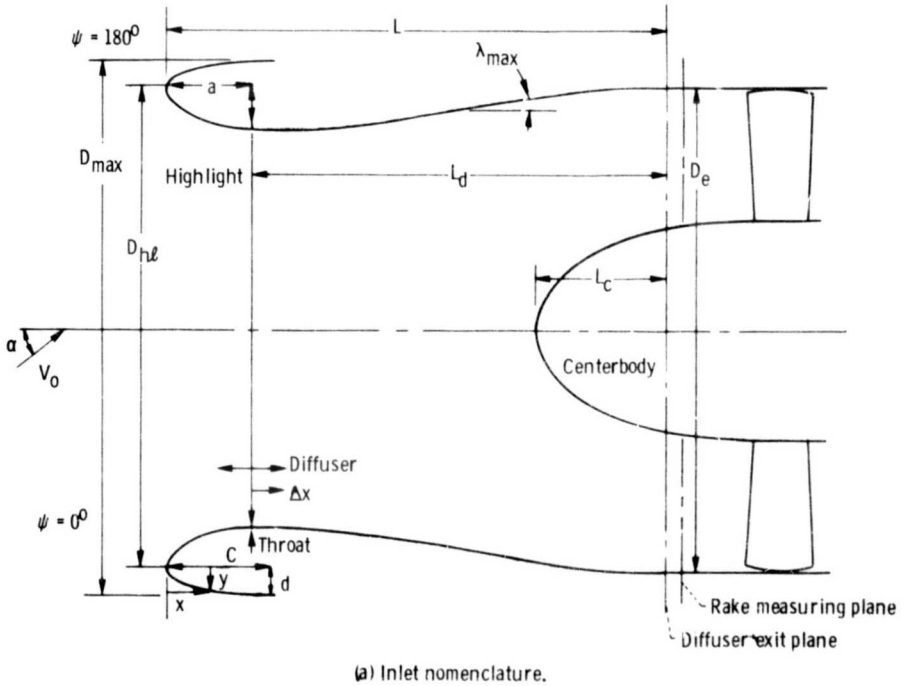

(a) Inlet nomenclature.

Figure 3. - Inlet designs.

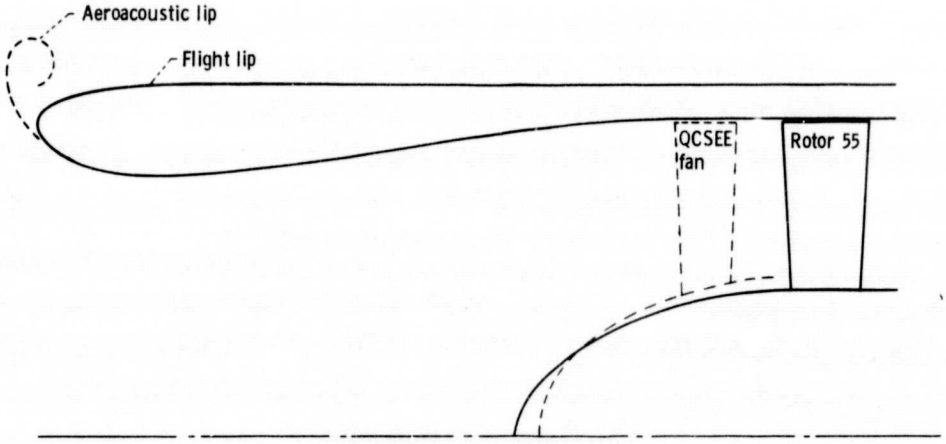

(b) Comparison of high Mach inlets.

Figure 3. - Concluded.

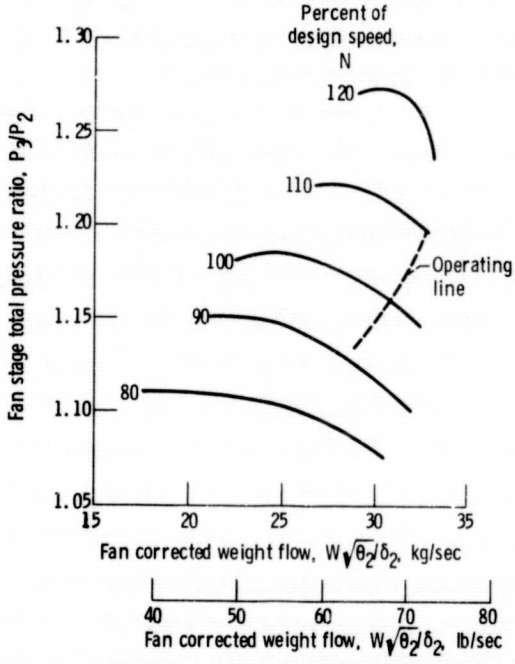

Figure 4. - Rotor 55 model fan performance.

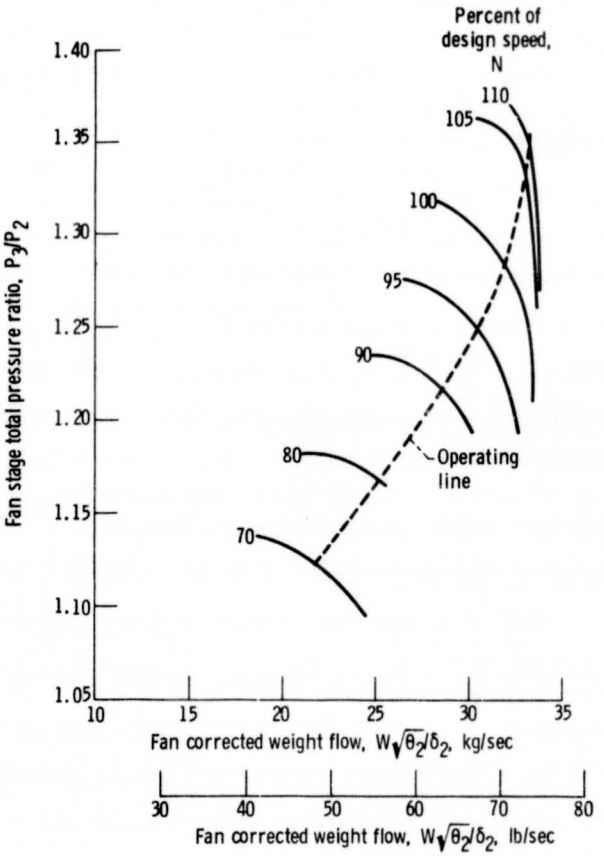

Figure 5. - QCSEE model fan performance.

Wind tunnel velocity, V_0, m/sec (knots)	STC calculation with $V_0 = 0$	
0	Flight lip	Open symbols
41 (80)	Aeroacoustic lip	Closed symbols

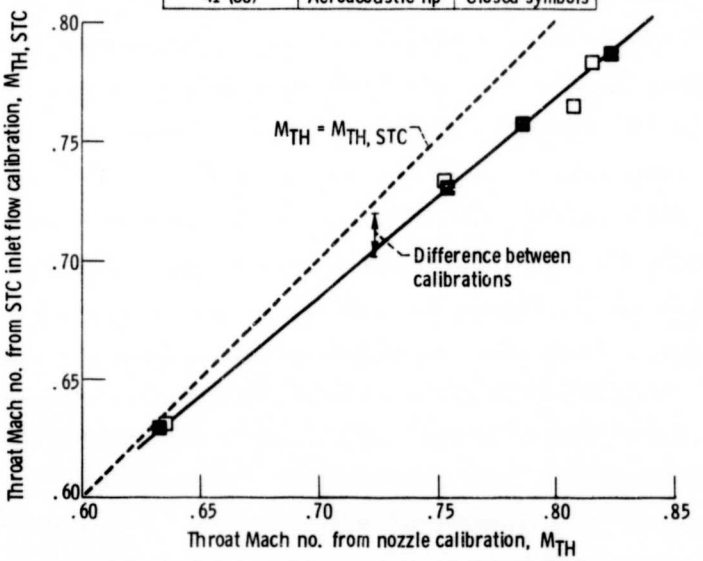

Figure 6. - Inlet HM throat Mach number correlation for the rotor 55 experiment.

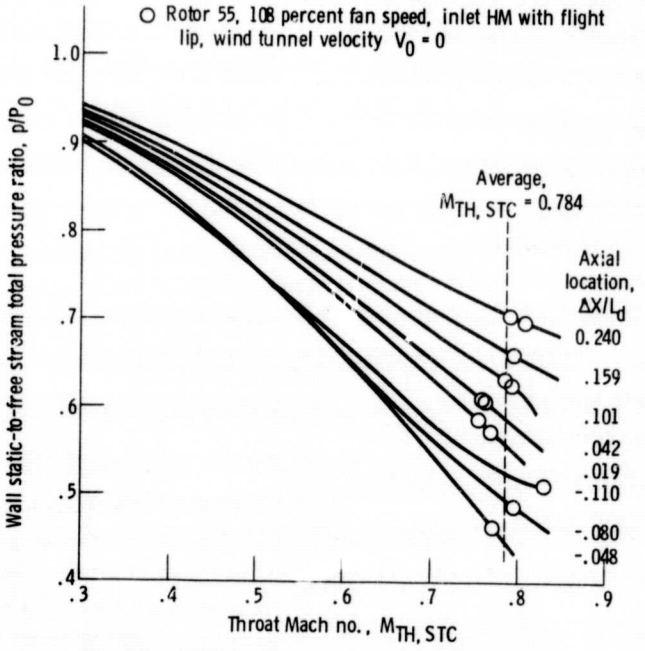

Figure 7. - Flight lip high Mach inlet STC flow correlation with boundary layer correction for wind tunnel velocity V_0 = 0.

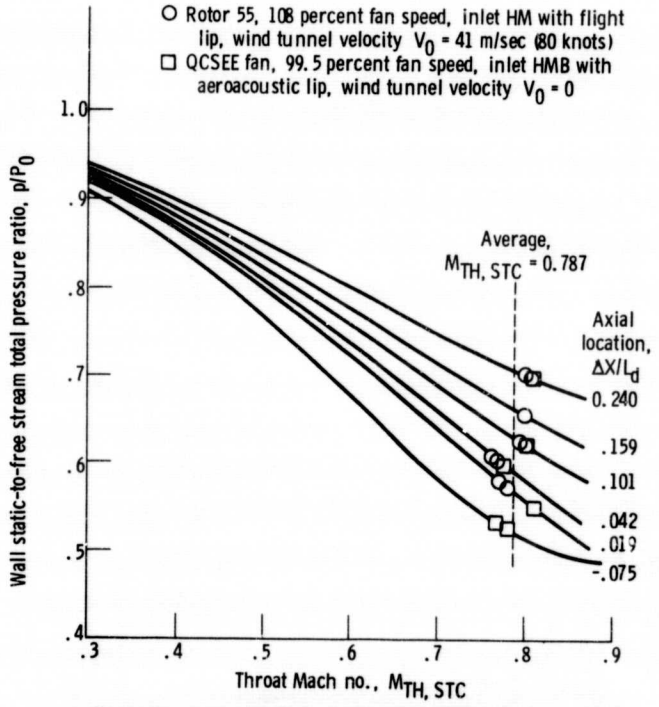

Figure 8. - Aeroacoustic lip high Mach inlet STC flow correlation with boundary layer correction for wind tunnel velocity V_0 = 0.

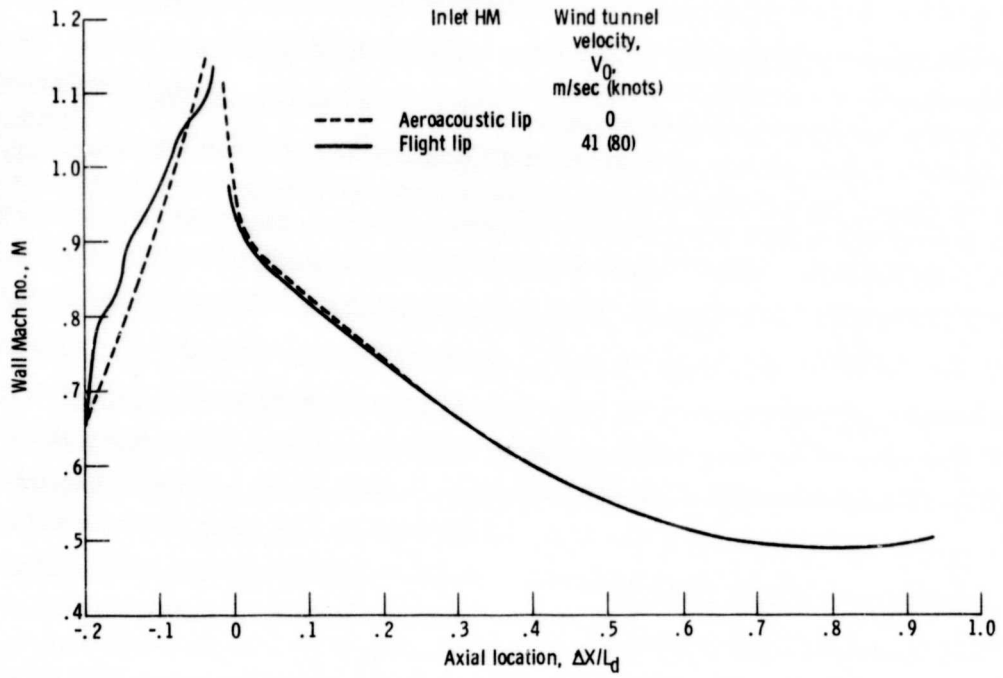

Figure 9. - inviscid STC flow calculations for throat Mach no. $M_{TH, STC} = 0.79$.

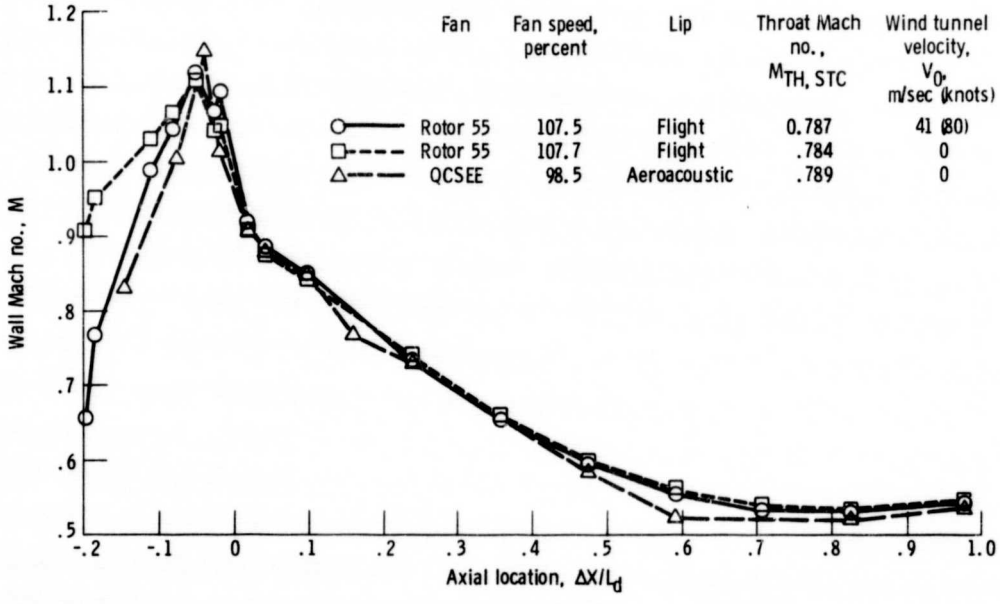

Figure 10. - Comparison of inlet HM wall Mach no. distributions.

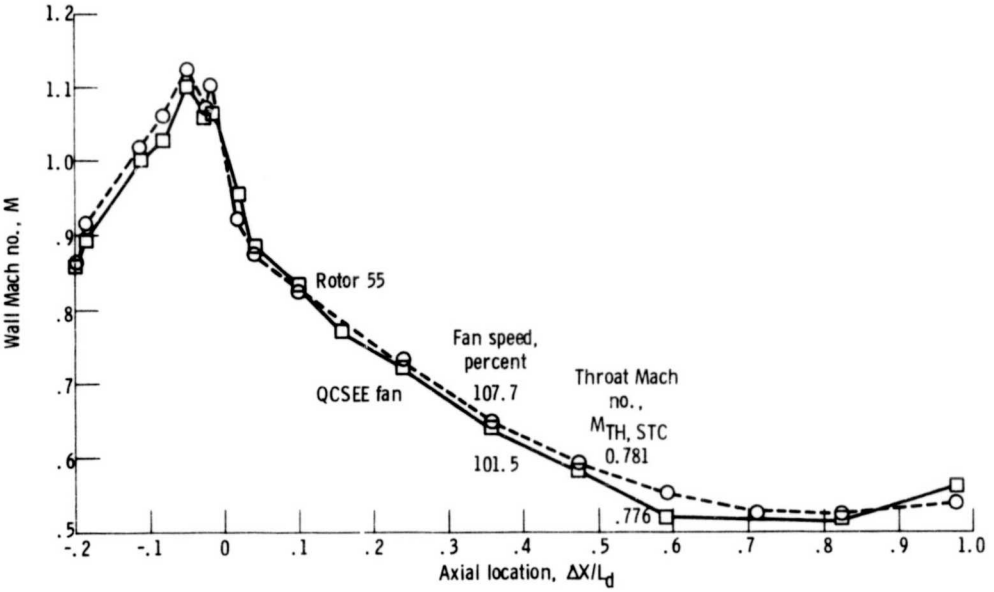

Figure 11. - Comparison of flight lip inlet HMB wall Mach no. distributions for wind tunnel velocity $V_0 = 0$.

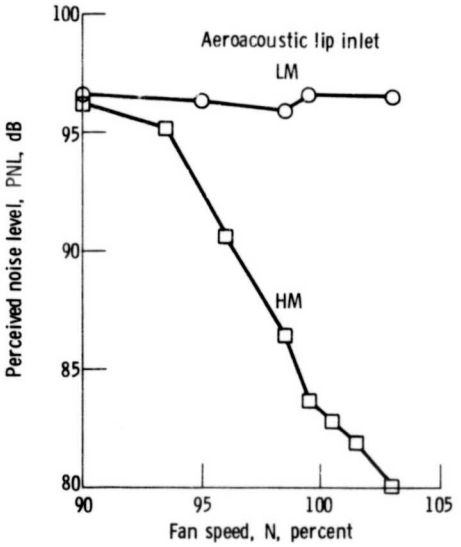

Figure 12. - Effect of fan speed on QCSEE fan perceived noise (engine scale, 152 M (500 ft) sideline, 60^0 from inlet centerline).

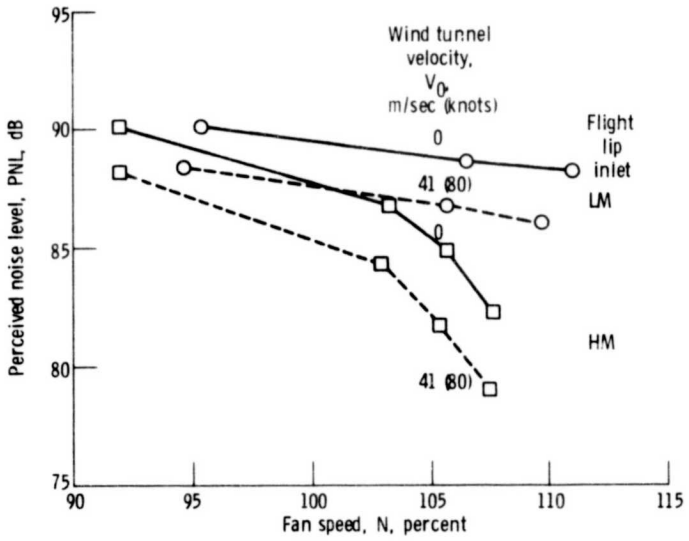

Figure 13. - Effect of fan speed on rotor 55 perceived noise (engine scale, 152 M (500 ft) sideline, 60° from inlet centerline).

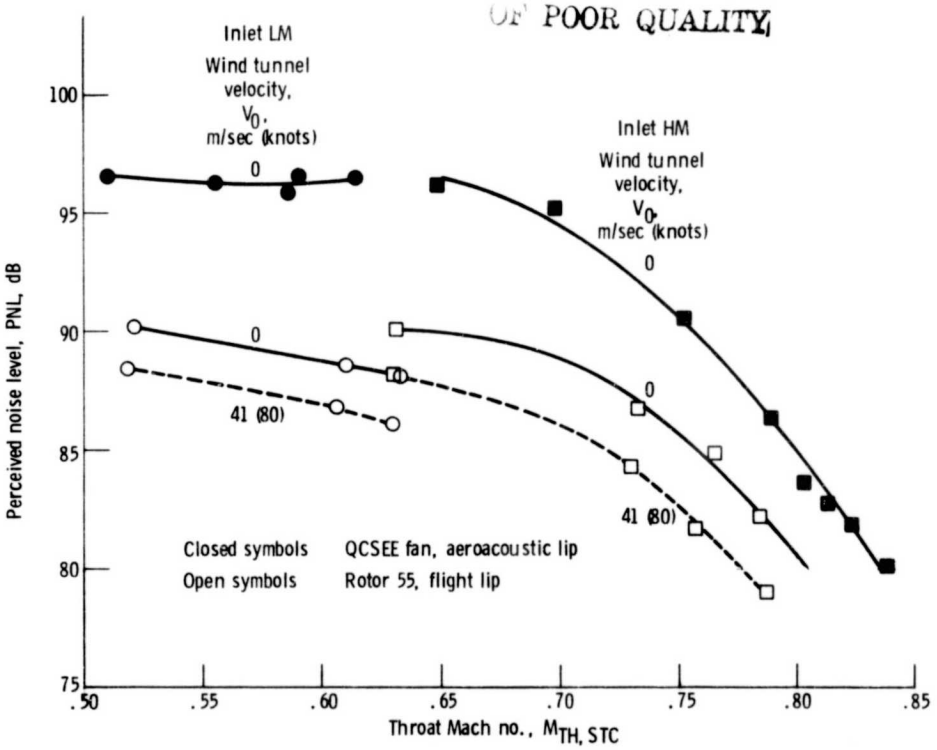

Figure 14. - Effect of inlet throat Mach no. on perceived noise (engine scale, 152 M (500 ft) sideline, 60° from inlet centerline).

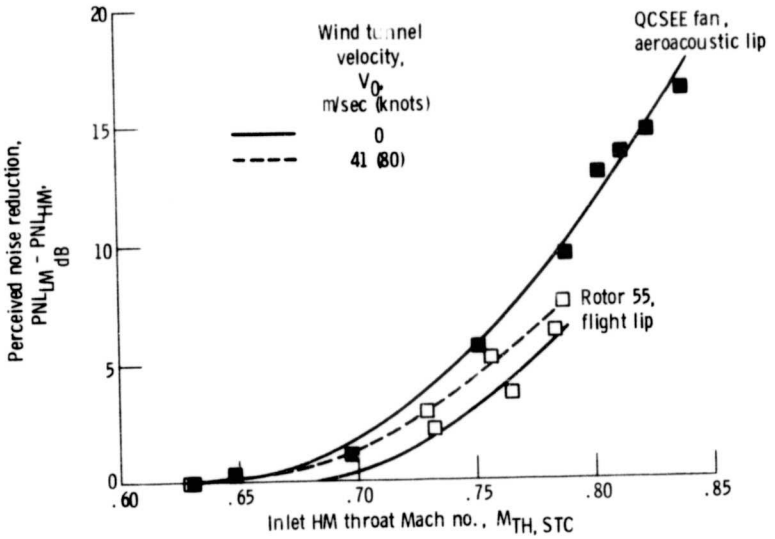

Figure 15. - Fan effect on inlet HM perceived noise reduction (engine scale, 152 M (500 ft) sideline, 60° from inlet centerline).

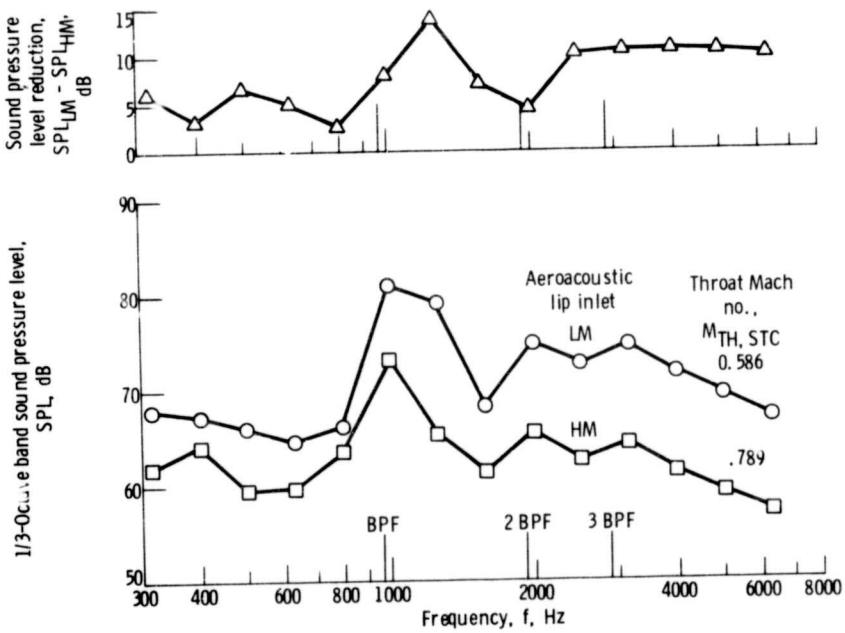

Figure 16. - QCSEE fan sound pressure level and reduction spectra (98.5 percent fan speed, engine scale, 152 M (500 ft) sideline, 60° from inlet centerline).

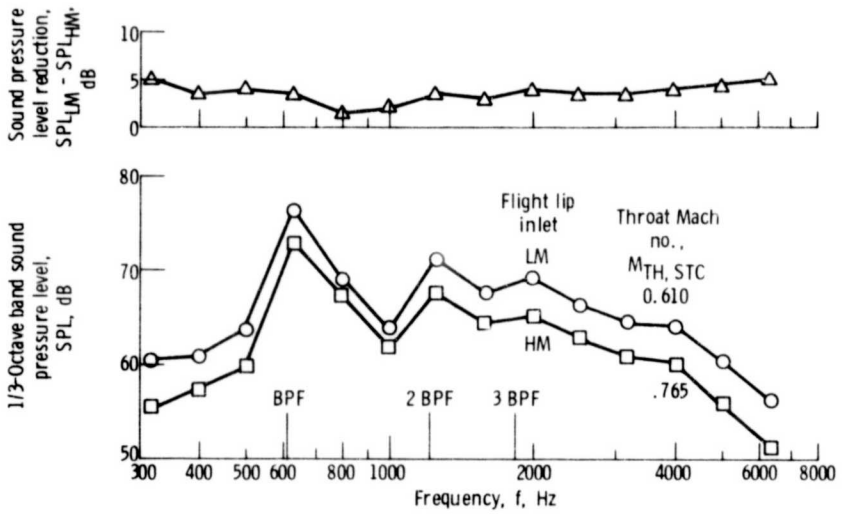

Figure 17. - Rotor 55 sound pressure level and reduction spectra with wind tunnel velocity V_0 = 0 (106 percent fan speed, engine scale, 152 M (500 ft) sideline, 60^0 from inlet centerline).

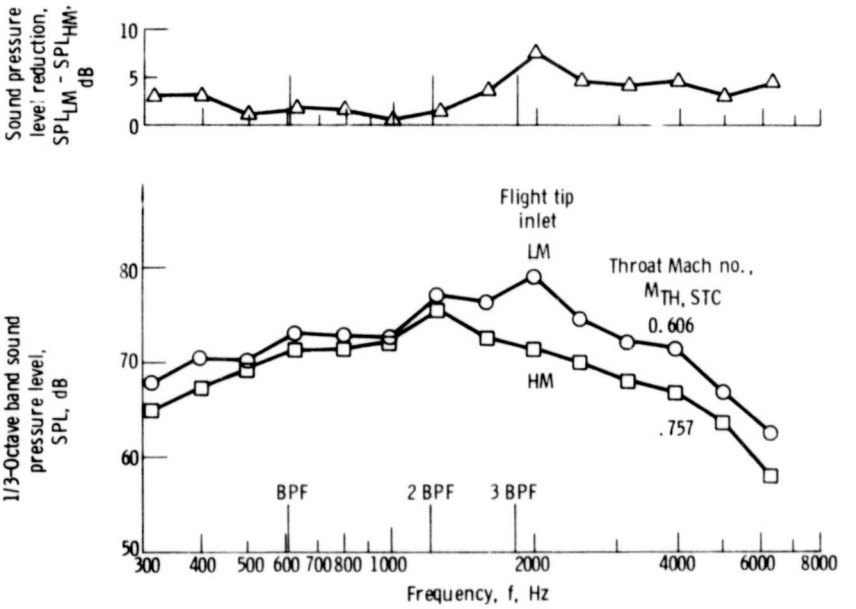

Figure 18. - Rotor 55 sound pressure level and reduction spectra with wind tunnel velocity V_0 = 41 m/sec (80 knots) (106 percent fan speed, engine scale, 152 M (500 ft) sideline, 60^0 from inlet centerline).